

Article

Seasonal Changes in Photosynthetic Energy Utilization in a Desert Shrub (*Artemisia ordosica* Krasch.) during Its Different Phenophases

Cai Ren ^{1,2} , Yajuan Wu ^{1,2}, Tianshan Zha ^{1,2,*}, Xin Jia ^{1,2}, Yun Tian ², Yujie Bai ², Charles P.-A. Bourque ^{2,3}, Jingyong Ma ² and Wei Feng ^{1,2}

¹ Yanchi Research Station, School of Soil and Water Conservation, Beijing Forestry University, Beijing 100083, China; cairenbjfu@foxmail.com (C.R.); yajuanwu2015@sina.com (Y.W.); xinjia@bjfu.edu.cn (X.J.); weifeng@bjfu.edu.cn (W.F.)

² Key Laboratory for Soil and Water Conservation, State Forestry Administration, Beijing Forestry University, Beijing 100083, China; tianyun@bjfu.edu.cn (Y.T.); bloweer@bjfu.edu.cn (Y.B.); cbourque@unb.ca (C.P.-A.B.); majy2015@bjfu.edu.cn (J.M.)

³ Faculty of Forestry and Environmental Management, 28 Dineen Drive, P.O. Box 4400, University of New Brunswick, Fredericton, NB E3B5A3, Canada

* Correspondence: tianshanzha@bjfu.edu.cn; Tel.: +86-10-6233-6608

Received: 26 February 2018; Accepted: 26 March 2018; Published: 29 March 2018



Abstract: Our understanding of the mechanisms of plant response to environment fluctuations during plants' phenological phases (phenophases) remains incomplete. Continuous chlorophyll fluorescence (ChlF) measurements were acquired from the field to quantify the responses in a desert shrub species (i.e., *Artemisia ordosica* Krasch. (*A. ordosica*)) to environmental factors by assessing variation in several ChlF-linked parameters and to understand plant acclimation to environmental stresses. Maximal quantum yield of PSII photochemistry (F_v/F_m) was shown to be reduced by environmental stressors and to be positively correlated to air temperature (T_a) during the early and late plant-growing stages, indicating a low temperature-induced inhibition during the leaf expansion and coloration phases. Effective quantum yield of PSII photochemistry (Φ_{PSII}) was negatively correlated to incident photosynthetically active radiation (PAR) irrespective of phenophase, suggesting excessive radiation-induced inhibition at all phenophases. The main mechanism for acclimating to environmental stress was the regulatory thermal dissipation (Φ_{NPQ}) and the long-term regulation of relative changes in Chl *a* to Chl *b*. The relative changes in photosynthetic energy utilization and dissipation in energy partitioning meant *A. ordosica* could acclimatize dynamically to environmental changes. This mechanism may enable plants in arid and semi-arid environments to acclimatize to increasingly extreme environmental conditions under future projected climate change.

Keywords: *Artemisia ordosica*; chlorophyll fluorescence; energy partitioning; phenophase; photoprotection

1. Introduction

Photosynthesis is a fundamental mechanism in plant metabolism that converts light energy into biochemical energy [1]. Excessive incident energy under high illumination usually leads to an accumulation of excitation pressure, which can impair photosystem II (PSII) and its associated light harvesting proteins, causing subsequent loss of PSII electron-transfer activity and finally inducing Photoinhibition [2–4].

Various tolerance and/or acclimation mechanisms exist in naturally grown plants to prevent damage to the photosynthetic apparatus from Photoinhibition [5]. For example, plants may (i) reduce

the absorbed incident radiation; (ii) regulate photo-protective thermal dissipation of absorbed energy by means of the xanthophyll cycle; and/or (iii) modulate the chlorophyll content and the ratio of chlorophyll *a* to chlorophyll *b* [6,7]. The assessment of Photoinhibition and its tolerance and/or acclimation can be accurately determined by a chlorophyll fluorescence (ChlF) measurement on a long time scale using mostly PAM fluorometers [8,9] and by a measurement of the OJIP fluorescence rise as reviewed, e.g., by Lazár [10]. A vast number of studies have shown that the activity of PSII and its associated light harvesting proteins gradually declined during the entire time of exposure to high illumination and that non-photochemical quenching (NPQ) increased in response to excessive radiation energy [11–13]. However, such inhibition of photosynthesis can not only arise from exposure to high light in the absence of other stresses, but also from too much light in the presence of other stresses that limit photosynthesis and thus, plant growth [14]. Studies on extreme temperatures suggested that heat stress significantly inhibited the maximal (F_v/F_m) and effective quantum yield of PSII photochemistry (Φ_{PSII}), and decreased the relative leaf chlorophyll content [15–17]. When facing low temperature stress, however, plants showed a sustained NPQ and improved photo-protection, which is associated with the reorganization of the light harvesting complex into aggregates [18,19]. Studies on water-deficit conditions showed a significant decrease in leaf chlorophyll concentration, whereas decreasing F_v/F_m was only observed during the more advanced stages of dehydration [20,21]. For natural conditions, both processes of absorption and utilization of photosynthetic energy are complicated when extreme temperatures, water status, and other stress factors become enmeshed [22]. On the other hand, acclimation of plants to a stressor (e.g., to high temperature) might cause some resistance against acute action of the stressor—see, e.g., Lazár et al. [23]. It is commonly observed that multiple stress factors in naturally growing plants synergistically reduce the photochemical rate and cause greater stress than what would have resulted from a single factor [24,25]. Further understanding of the mechanisms associated with photosynthetic tolerance and/or acclimation to multiple stressors is needed for naturally growing plants, particularly for desert plants.

Deserts cover ~15% of the terrestrial surface and have been rapidly expanding due to climate change and human practices [26,27]. Cold-desert ecosystems are characterized by harsh environments and strong hydrometeorological gradients [28]. The absorption and utilization of photosynthetic energy by cold-desert plants are usually inhibited by high illumination, extreme temperature, water deficits, and other climatic irregularities [29]. Thus, plants in cold-desert ecosystems may produce lower amounts of photosynthate and tend to exhibit lower resilience and resistance to disturbances of similar severity than plants in environmentally-moderate ecosystems [30]. Most of the existing studies have focused on plants of the Mediterranean region and North America, where ecosystems are characterized by cold–wet winters and hot–dry summers [31,32]. The cold-desert regions in semi-arid China, however, differed climatically by having cold–dry winters and hot–wet summers due to the impact of the monsoon season, which could lead to different stress conditions. Spring and summer droughts are mostly common stresses in this region [33,34]. Cold-desert plant responses to environmental stress would provide additional insight into the mechanistic understanding of photosynthetic energy utilization by terrestrial plants.

Artemisia ordosica Krasch. (hereafter, *A. ordosica*), a long-lived, deciduous woody shrub species, is naturally dispersed throughout the Mu Us desert [35]. It is the main species providing wind and sand protection in arid- and semi-arid areas of northwest China. *A. ordosica* usually buds in early April and accumulates its greatest biomass in June, slowing its growth from July to defoliating in October [36]. The functional responses of *A. ordosica* are known to vary with plant phenological phases (or phenophases [37]) as diverse environmental conditions induce differential photochemical responses in photosynthetic apparatus [38]. We hypothesized that photosynthetic energy utilization of a cold-desert plant in response to environmental stress differs seasonally and varies as a function of phenophase. To test our hypothesis, ChlF of *A. ordosica* was measured continuously in situ during the growing season of 2014. The specific objectives of the study were to: (1) examine temporal dynamics of several ChlF-associated parameters and their responses to environmental factors during different

phenophases; and (2) to understand the mechanisms associated with defining the species' tolerance and acclimation to environmental stresses in relation to its phenophases.

2. Materials and Methods

2.1. Site Characteristics

The experimental site is located in the Yanchi Desert Ecosystem Research Station (37.68° N to 37.73° N, 107.20° E to 107.26° E, 1570 m a.s.l.), northwestern China. The site is in a transitional region between the southern Mu Us desert and northern Loess plateau. It belongs to a mid-temperate, semi-arid region with a continental monsoon climate. From 1954 to 2004, the region's mean annual air temperature was 8.1 °C. The mean T_a from spring to autumn was 9.3, 21.3, and 7.7 °C, respectively [39]. Mean annual precipitation (PPT) was 287 mm, showing large seasonal (~80% falling during the June–September period) and inter-annual variation (133–572 mm year⁻¹). The area's soil type is classified as a sierozem, with >70% fine sand (0.02–0.20 mm). Mean annual potential evapotranspiration is >PPT. Subsurface water levels lie between 8–10 m from the ground surface and is currently decreasing. The dominant native shrub species of the region is *A. ordosica*.

2.2. Environmental Measurements

Environmental factors were measured simultaneously over the growing season from 12 April to 12 October 2014, including (1) photosynthetically active radiation (PAR) with a quantum sensor (PAR-LITE, Kipp and Zonen, Delft, The Netherlands); air temperature (T_a) and relative humidity (RH) with a thermohygrometer (HMP155A, Vaisala, Vantaa, Finland); soil water content (SWC) with ECH2O-5TE sensors (Decagon Devices, Pullman, WA, USA) set at depths of 10, 30, and 70 cm into the soil; and PPT with a tipping bucket rain gauge (TE525WS, Campbell Scientific Inc., Logan, UT, USA). All meteorological variables were measured every 10 s, and averaged or summed to generate 30-min values before being stored on data loggers (CR200X for PPT, CR3000 for all others, Campbell Scientific Inc.). Half-hourly values of vapor pressure deficit (VPD), representing air dryness, were calculated as defined by Wilhelm et al. [40]

$$\text{VPD} = e - e \times \frac{\text{RH}}{100} \quad (1)$$

$$e = 0.611 \times \exp \frac{17.27 T_a}{237.3 + T_a} \quad (2)$$

where e is the partial water vapor pressure at the point of saturation.

Phenological observations were made using photographs taken twice each week. Phenophases include three obvious phases, i.e., (i) leaf-expanding phase during day of year (DOY) 102–147; (ii) leaf-expanded phase during DOY 148–247; and (iii) leaf-coloring phase during DOY 238–285. For details concerning phenological observations at the site, consult Chen et al. [41].

Chlorophyll a and b content were measured approximately once per week using spectrophotometry, UV-2100 (UNICO, China). Fresh south-facing leaves were collected from nearby plants similar to those being sampled. Two grams of clean leaves were weighed, ground into a powder with a small amount of quartz sand and calcium carbonate added. The powder was dissolved into a turbid fluid with dehydrated ethanol. The turbid fluid was subsequently filtered and calibrated to a volume of 200 mL. Finally, aqueous-chlorophyll extract was subsequently injected into a spectrophotometer using the energy spectrum from 645 to 663 nm to assess chlorophyll content. The values of chlorophyll content (ChlC, mg g⁻¹) and the ratio of chlorophyll a to chlorophyll b content (Chl a/b) were calculated with a modified Arnon equation set [42,43], i.e.,

$$\text{Chl } a = (12.71A_{663} - 2.59A_{645}) \times \frac{V}{1000 \times W} \quad (3)$$

$$\text{Chl } b = (22.88A_{645} - 4.67A_{663}) \times \frac{V}{1000 \times W} \quad (4)$$

$$\text{Chl } C = \text{Chl } a + \text{Chl } b \quad (5)$$

$$\text{Chl } a/b = \text{Chl } a / \text{Chl } b \quad (6)$$

where A_{663} and A_{645} are the light absorption at 663 and 645 nm, respectively, V (mL) is the volume of the extract, and W (g) is the weight of fresh leaves.

2.3. ChlF Measurements, Data Treatment, and Analysis

Field measurements of ChlF parameters were made from three fully-grown *A. ordosica* plants, which averaged 50 cm in height and 80×60 cm in canopy size. Three Monitoring-PAM detectors (MONI-head; Walz, Effeltrich, Germany) were individually set on a fascicle of randomly chosen leaves (~12 leaves) in the middle of south-facing stems on each of three sampled shrubs. Three detector heads represent three replicates of the same measurement. ChlF-associated parameters (i.e., effective and maximum fluorescence values, F' and $F_{m'}$, respectively) were recorded with modulated light pulses. The actinic light driving photosynthesis was the light from the Sun. The time interval between measurements was 10 min. Measurements were stored in memory of the PAM analyzer (MONI-DA). The PAM system was powered by a solar panel.

From the two basic fluorescence parameters (i.e., F' and $F_{m'}$), defined by the mean of three replicate, simultaneous measurements, other parameters can be calculated [44]. Effective quantum yield of PSII photochemistry (Φ_{PSII} , Equation (7)) is a light-adapted parameter that reflects the effective portion of absorbed quanta used in PSII. Maximal quantum yield of PSII photochemistry (F_V/F_m , Equation (8)) is a dark-adapted parameter, which estimates the maximum portion of absorbed quanta used in PSII. Stern–Volmer non-photochemical fluorescence quenching (NPQ, Equation (9)) is a parameter that reflects heat-dissipation of excitation energy [45]. The three ChlF-associated parameters were calculated as

$$\Phi_{\text{PSII}} = \frac{F_{m'} - F'}{F_{m'}} \quad (7)$$

$$F_V/F_m = \frac{F_m - F_0}{F_m} \quad (8)$$

$$\text{NPQ} = \frac{F_m - F_{m'}}{F_{m'}} \quad (9)$$

where F' is the steady-state fluorescence in ambient light and $F_{m'}$ is the maximum fluorescence in ambient light following a saturating light pulse. The intensity of the measuring light and the saturating pulses were $0.9 \mu\text{mol m}^{-2} \text{s}^{-1}$ and $3500 \mu\text{mol m}^{-2} \text{s}^{-1}$, respectively. Daytime F' and $F_{m'}$ become nighttime F_0 and F_m . Nighttime was defined as the period with $\text{PAR} < 5 \mu\text{mol m}^{-2} \text{s}^{-1}$ [46,47].

The approach of energy partitioning was introduced and developed by researchers (i.e., Genty, Cailly, Kramer, Hendrickson, etc.; [48–51]) to discriminate different types of non-photochemical losses [52]. Parameter Φ_{NPQ} is the quantum yield of regulatory (light-induced) non-photochemical quenching that represents thermal dissipation related to all photo-protective mechanisms, whereas Φ_{NO} is the quantum yield of constitutive non-regulatory (basal or dark) energy dissipation, which represents all other components of non-photochemical quenching that are not photo-protective [52], i.e.,

$$\Phi_{\text{NO}} = \frac{1}{\text{NPQ} + 1 + qL \left(\frac{F_m}{F_0} - 1 \right)} \quad (10)$$

$$\Phi_{\text{NPQ}} = 1 - \Phi_{\text{PSII}} - \Phi_{\text{NO}} \quad (11)$$

where qL is coefficient of photochemical quenching in the lake model, which is taken to describe the energetic connectivity in terrestrial plants, which is a better estimate than that provided in the puddle

model, as reviewed by Lazár [53]. Parameter $F_{o'}$ is the minimal fluorescence in light-adapted conditions, representing F_o with non-photochemical quenching [54]. Both parameters were calculated as

$$qL = \frac{F_{m'} - F'}{F_{m'} - F_{o'}} \left(\frac{F_{o'}}{F'} \right) \quad (12)$$

$$F_{o'} = \frac{F_o}{\frac{F_v}{F_m} + \frac{F_o}{F_{m'}}} \quad (13)$$

Rainy days were removed from the analysis to avoid rainfall-pulse disturbances. A Pearson correlation analysis over the entire growing season was conducted in MATLAB (MathWorks, Natick, MA, USA), largely to quantify correlations between ChlF-associated parameters and meteorological factors. Generalized linear regression was used to quantify response sensitivity during each phenophase [46]. Multivariate stepwise regression was used to further analyze interaction between individual meteorological factors on ChlF-associated parameters [32].

3. Results

3.1. Phenological Dynamics in Biophysical Factors

Daily-integrated PPT, daily means of PAR, T_a , RH, and SWC at three soil depths showed distinct patterns for the different phenophases (Figure 1). Daily mean PAR increased from 108.0 $\mu\text{mol m}^{-2} \text{s}^{-1}$ (DOY 108) during the early leaf-expanding phase to a maximum of 591.0 $\mu\text{mol m}^{-2} \text{s}^{-1}$ (DOY 195) during the leaf-expanded phase, and then decreased to 98.6 $\mu\text{mol m}^{-2} \text{s}^{-1}$ (DOY 284) during the late leaf-coloring phase (Figure 1a). Daily mean T_a increased from 8.6 °C (DOY 108) during the early leaf-expanding phase to a maximum of 25.8 °C (DOY 214) during the leaf-expanded phase, and then decreased to 3.5 °C (DOY 284) during the late leaf-coloring phase (Figure 1b). Daily mean RH decreased from 49.9% (DOY 102) during the early leaf-expanding phase to a minimum of 13.8% (DOY 147) during the late leaf-expanding phase, and increased to 80% during the leaf-expanded and coloring phases (Figure 1b). Daily mean VPD varied in a manner similarly observed to that of T_a (Figure 1c). Total PPT during the observation period was 295.9 mm. Rainy days occurred about 24% of the time (11 of 45 days), 40% (31 of 77 days), and 48% (23 of 48 days) during the leaf-expanding, expanded, and coloring phases, respectively. Concomitant PPT-amounts during the three phenophases accounted for 9.3, 52.0, and 38.7% of the total PPT falling during the growing season (Figure 1d). Soil water content at a soil depth of 10 and 30 cm responded instantly to rain pulses exceeding 5 mm. The response decreased with an increase in soil depth during the growing season, and showed nominal fluctuation ($<0.01 \text{ m}^3 \text{ m}^{-3}$) at depths ≥ 70 cm (Figure 1d). In general, the annual mean of each of meteorological parameters was basically close to its multi-year average. The leaf-expanding phase occurred during a dry and cold period, and the leaf-expanded phase occurred during a high radiation period. Leaf coloring, in contrast, occurred during rainy and cold conditions.

3.2. Phenological Variations in ChlF Parameters

Figure 2 shows the seasonal dynamics of ChlF-associated parameters in vivo. Daily mean F_v/F_m increased from a minimum of 0.66 (DOY 107) to 0.78 during the leaf-expanding phase, then decreased to 0.67 (DOY 190), and fluctuated at 0.76 subsequently (Figure 2a), averaging 0.71 ± 0.08 , 0.76 ± 0.03 , 0.76 ± 0.03 (\pm standard deviation) during the leaf-expanding, expanded, and coloring phases, respectively. Daily mean Φ_{PSII} demonstrated a similar trend to that observed with F_v/F_m , with low values occurring in the early leaf-expanding and leaf-expanded phases (Figure 2b). The seasonal pattern in ChlC was consistent with the pattern observed in F_v/F_m ; Chl a/b varied in an opposite direction from that of ChlC (Figure 2c,d). A drastic change of ChlC and Chl a/b occurred from DOY 210 to 240, after which Chl a/b increased to a maximum of 6.0 (DOY 284) during the late leaf-coloring phase (Figure 2c,d).

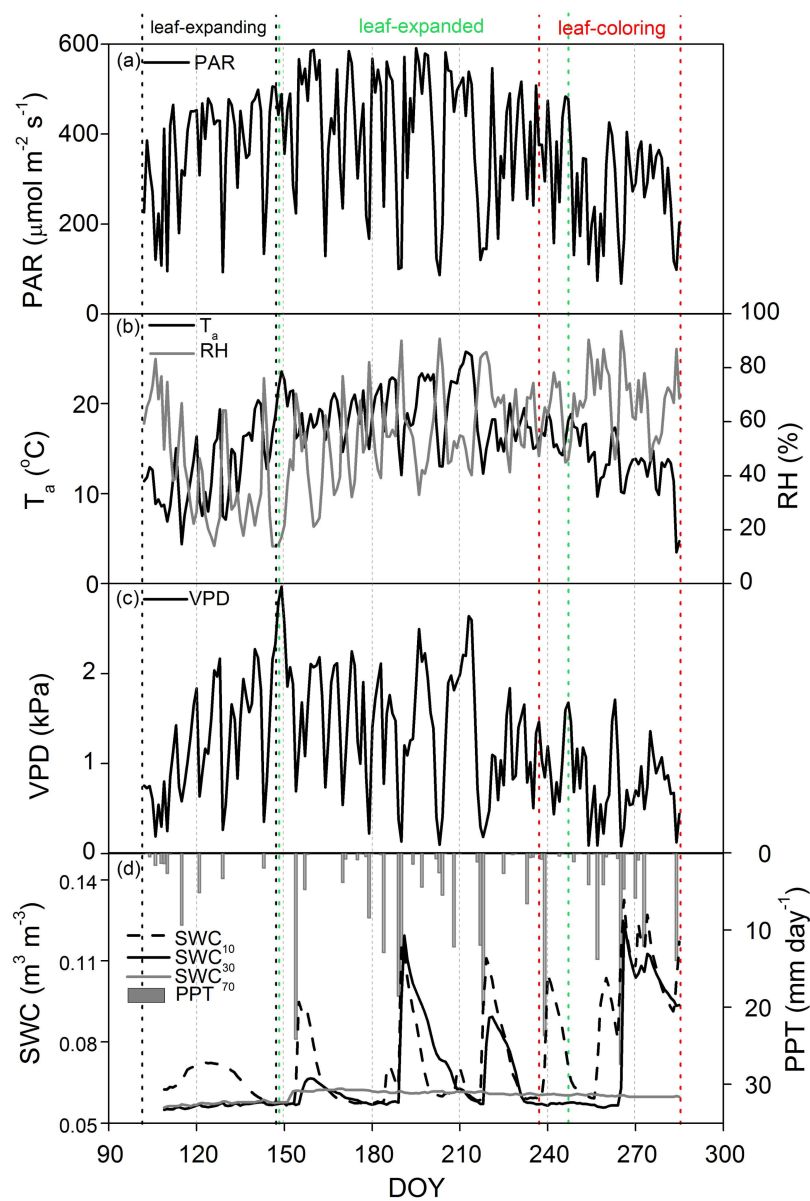


Figure 1. Time series of meteorological variables: daily mean incident photosynthetically active radiation (PAR, (a)), air temperature (T_a , (b)), relative humidity (RH, (b)), atmospheric vapor pressure deficit (VPD, (c)), soil water content (SWC, (d)) at three soil depths (10, 30, and 70 cm), and daily-cumulated rainfall (PPT, (d)) during the growing season (DOY 102 to 285) of 2014. Black, green, and red vertically dotted lines represent leaf-expanding, expanded, and coloring phenophases.

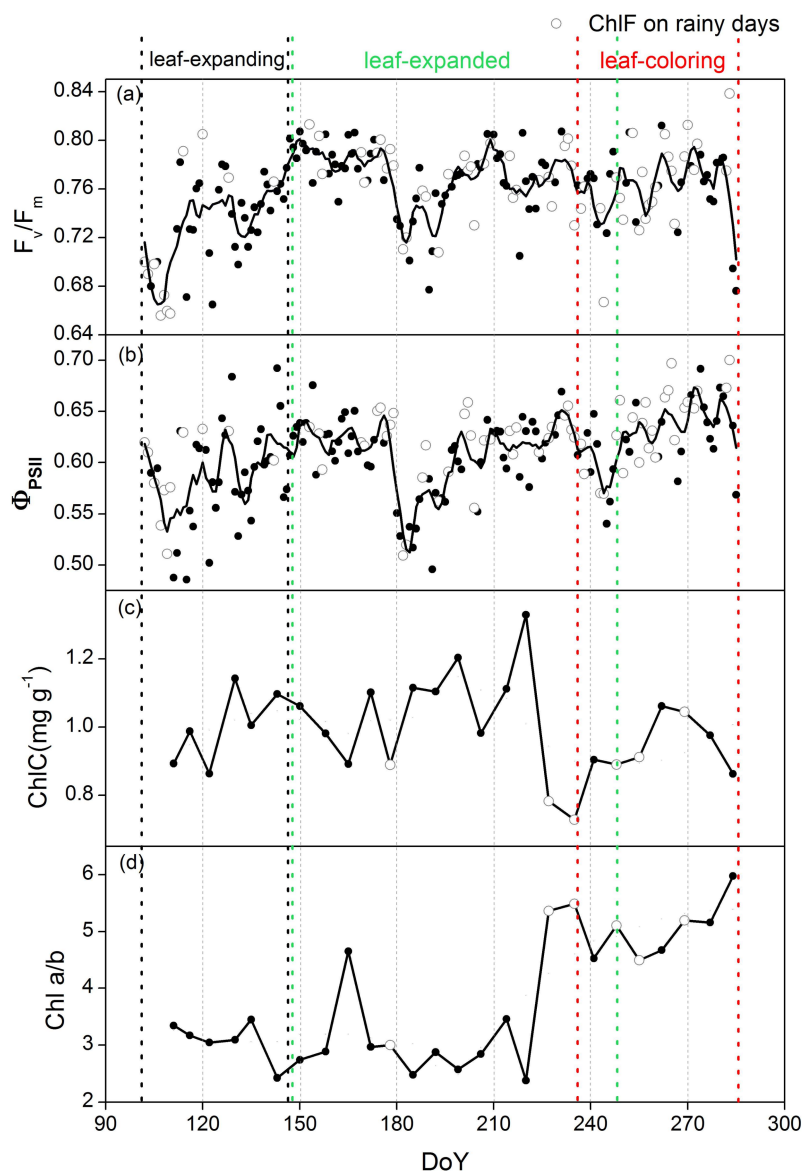


Figure 2. Time series of ChlF-associated parameters, i.e., maximal quantum yield of PSII photochemistry (F_v/F_m , (a)), daily mean effective quantum yield of PSII photochemistry (Φ_{PSII} , (b)), sum content of chlorophyll a and b (ChlC, (c)), and ratio of chlorophyll a to chlorophyll b (Chl a/b, (d)) during the growing season (DOY 102 to 285) of 2014. Open circles represent ChlF-associated parameter values during rainy days. Major trend lines for F_v/F_m and Φ_{PSII} were modified according to the Savitzky-Golay method. Black, green, and red vertically dotted lines represent leaf-expanding, expanded, and coloring phenophases.

3.3. Proportion of Energy Partitioning and Response of ChlF to Abiotic Factors

Daily response of ChlF was modified by different meteorological factors. Generally, F_v/F_m increased with increasing daily mean of T_a during the leaf-expanding and coloring phases (Figure 3a). The slopes of F_v/F_m -to- T_a regressions for the leaf-expanding phase were similar to those observed for the leaf-coloring phase (Table 1). Multivariate regressions confirmed T_a as the main controlling factor of F_v/F_m during both phenophases (Table 2). Regression of ChlF with ChlC as independent variable showed that ChlC was positively correlated to F_v/F_m during the leaf-expanding and coloring phases (Figure 3b).

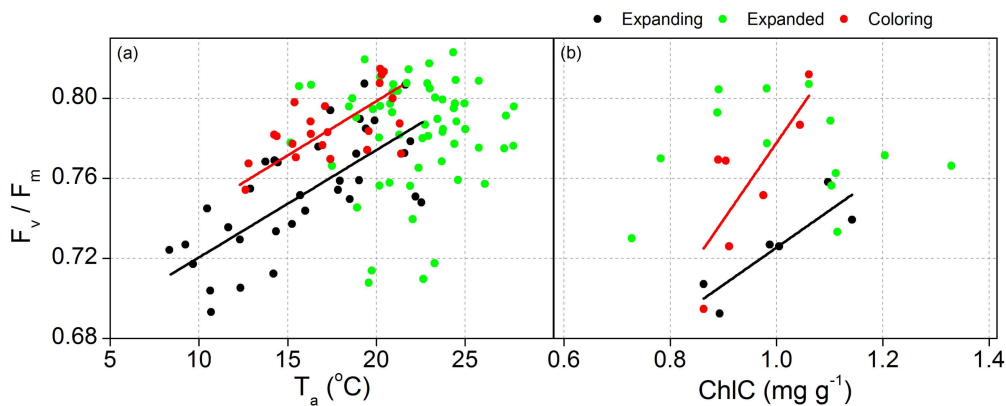


Figure 3. Relationship between maximal quantum yield of PSII photochemistry (F_v/F_m) and daily mean air temperature (T_a , (a)), and the sum content of chlorophyll *a* and chlorophyll *b* (ChlC, (b)) during each phenophase for the 2014 growing season. Black, green, and red colored circles and lines coincide with values and fitting functions (Table 1) for the leaf-expanding, expanded, and coloring phases, respectively. Data from rainy days were excluded from the analysis.

Table 1. Regression equations between meteorological variables and ChlF-associated parameters during the growing season (DOY 102 to 285) of 2014. Independent variables include daily mean incident photosynthetically active radiation (PAR), air temperature (T_a), relative humidity (RH), atmospheric vapor pressure deficit (VPD), sum content of chlorophyll *a* and chlorophyll *b* (ChlC), and ratio of chlorophyll *a* to chlorophyll *b* (i.e., Chl *a/b*). Dependent variables include maximal quantum yield of PSII photochemistry (F_v/F_m), daily mean effective quantum yield of PSII photochemistry (Φ_{PSII}), Stern–Volmer non-photochemical fluorescence quenching (NPQ), and quantum yield of regulatory light-induced non-photochemical quenching (Φ_{NPQ}). *p*-values represent significant level for the regression models. r^2 is the coefficient of determination.

	Factors	Phase	Equation	r^2	<i>p</i>
F_v/F_m	T_a	Expanding	$y = 0.67 + 53.7 \times 10^{-4}x$	0.51	<0.05
		Coloring	$y = 0.69 + 54.3 \times 10^{-4}x$	0.50	0.01
	ChlC	Expanding	$y = 0.54 + 0.19x$	0.71	0.02
		Coloring	$y = 0.39 + 0.38x$	0.52	0.04
Φ_{PSII}	T_a	Expanding	$y = 0.52 + 45.9 \times 10^{-4}x$	0.25	0.02
	PAR	Expanding	$y = 0.67 - 1.81 \times 10^{-4}x$	0.14	0.02
		Expanded	$y = 0.67 - 1.29 \times 10^{-4}x$	0.17	<0.05
		Coloring	$y = 0.72 - 2.45 \times 10^{-4}x$	0.44	<0.05
NPQ	Chl <i>a/b</i>	Expanding	$y = 2.70 - 0.68x$	0.78	0.01
		Expanded	$y = 1.06 - 0.12x$	0.30	0.02
Φ_{NPQ}	RH	Expanding	$y = 22.85 - 0.18x$	0.34	<0.05
		Expanded	$y = 23.73 - 0.09x$	0.14	<0.05
	VPD	Expanding	$y = 11.82 + 4.20x$	0.25	<0.05
		Expanded	$y = 15.99 + 2.44x$	0.15	<0.05
		Coloring	$y = 11.26 + 4.96x$	0.41	<0.05
	PAR	Expanding	$y = 4.23 + 0.03x$	0.48	<0.05
		Expanded	$y = 9.84 + 0.02x$	0.42	<0.05
		Coloring	$y = 6.87 + 0.03x$	0.58	<0.05

Table 2. Multi-variate linear regressions between meteorological variables and ChlF-associated parameters during the growing season (DOY 102 to 285) of 2014. Independent variables include daily mean incident photosynthetically active radiation (PAR), air temperature (T_a), relative humidity (RH), and atmospheric vapor pressure deficit (VPD). Dependent variables include maximal quantum yield of PSII photochemistry (F_v/F_m), daily mean effective quantum yield of PSII photochemistry (Φ_{PSII}), and quantum yield of regulatory light-induced non-photochemical quenching (Φ_{NPQ}). p -values represent significant level for the regression models. r^2 is the coefficient of determination.

	Factors	Phase	Equation	r^2	p
F_v/F_m	T_a	Expanding	$y = 56.77 \times 10^{-4}x + 0.66$	0.45	<0.01
		Expanded	-	-	-
		Coloring	$y = 30.14 \times 10^{-4}x + 0.73$	0.26	0.01
Φ_{PSII}	PAR (x_1), T_a (x_2) VPD(x_3)	Expanding	$y = -3.54 \times 10^{-4}x_1 + 78.34 \times 10^{-4}x_2 + 0.61$ ($-0.70x_1 + 0.85x_2$ in standardized form)	0.67	<0.01
		Expanded	$y = -2.22 \times 10^{-4}x_1 + 314.6 \times 10^{-4}x_3 + 0.66$ ($-0.70x_1 + 0.49x_3$ in standardized form)	0.31	<0.01
		Coloring	-	-	-
Φ_{NPQ}	PAR	Expanding	$y = 0.026x + 7.73$	0.32	<0.01
		Expanded	$y = 0.016x + 13.02$	0.28	<0.01
		Coloring	$y = 0.023x + 8.44$	0.46	<0.01

Daily mean Φ_{PSII} increased with increasing T_a during the leaf-expanding phase (Figure 4a), but decreased with increasing PAR irrespective of phenophase (Figure 4b). The slope of the Φ_{PSII} -to-PAR relationship was lowest during the leaf-expanded phase (Table 1). Multivariate regressions indicated that the relative effect of PAR on Φ_{PSII} was small than that of T_a during the leaf-expanding phase (standardized coefficient of -0.70 for PAR vs. 0.85 for T_a), but larger than that of VPD during the leaf-expanded phase (standardized coefficient of -0.70 for PAR vs. 0.49 for VPD; Table 2). Chl a/b was negatively correlated to NPQ during the leaf-expanding and expanded phases (Figure 5).

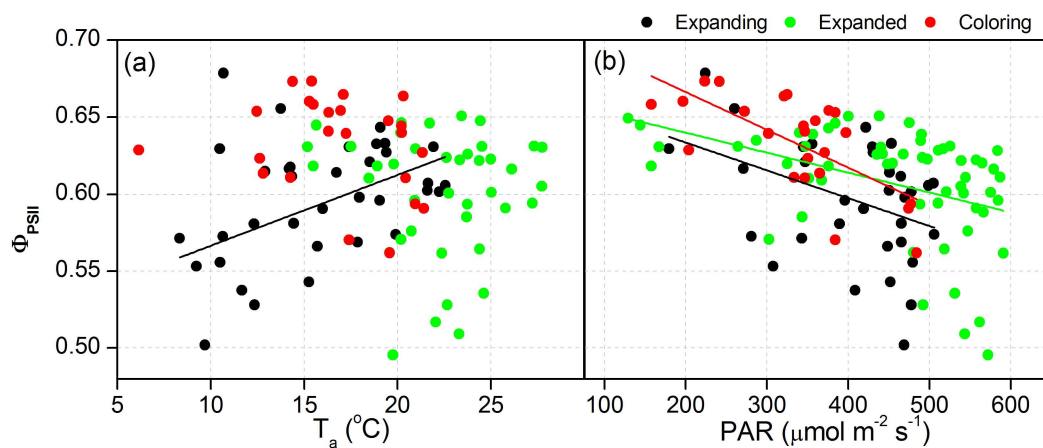


Figure 4. Relationship between daily mean effective quantum yield of PSII photochemistry (Φ_{PSII}), daily mean air temperature (T_a , (a)), and incident photosynthetically active radiation (PAR, (b)) during each phenophase during the 2014 growing season. Black, green, and red colored circles and lines coincide with values and fitting functions (Table 1) for the leaf-expanding, expanded, and coloring phases, respectively. Data from rainy days were excluded from the analysis.

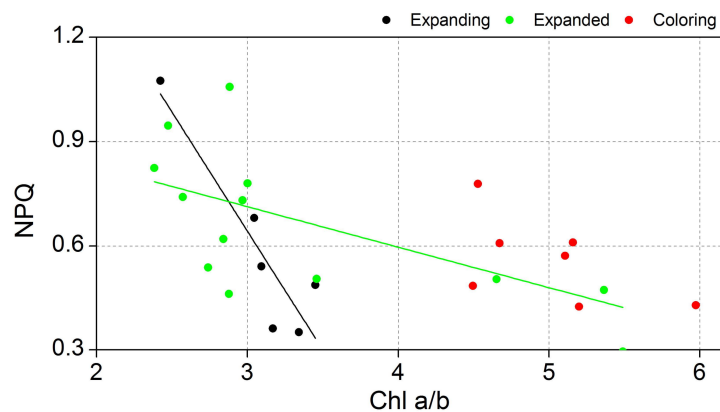


Figure 5. Relationship between Stern–Volmer non-photochemical fluorescence quenching (NPQ) and the ratio of chlorophyll a to chlorophyll b content (i.e., Chl a/b) in each phenophase during the 2014 growing season. Black, green, and red colored circles and lines coincide with values and fitting functions (Table 1) for the leaf expanding, expanded, and coloring phases, respectively. Data from rainy days were excluded from the analysis.

Figure 6 shows the dynamics of energy partitioning in PSII. The energy partitioning of Φ_{PSII} ranged from 48.6% to 71.4%, 49.6% to 67.6%, and 54.0% to 70.0% during the leaf-expanding, expanded and coloring phases, respectively, averaging $59.3 \pm 5.2\%$, $60.3 \pm 3.9\%$, and $63.0 \pm 3.8\%$ (\pm standard deviation). The proportion of Φ_{NPQ} increased from 10% (DOY 107) during the early leaf-expanding phase to a maximum level of 25.0% (DOY 190), and declined to 10% (DOY 284) during the late leaf-coloring phase, averaging $16.3 \pm 5.7\%$, $18.7 \pm 3.9\%$, and $15.4 \pm 3.7\%$ during the three phenophases, respectively. Parameter Φ_{NPQ} exhibited greater variance (i.e., larger standard deviations) during the leaf-expanding phase. Days with Φ_{NO} within the range of 20–30% accounted for 74% (34 of 46 days), 94.8% (73 of 77 days), and 95.8% (46 of 48 days) during the three phenophases.

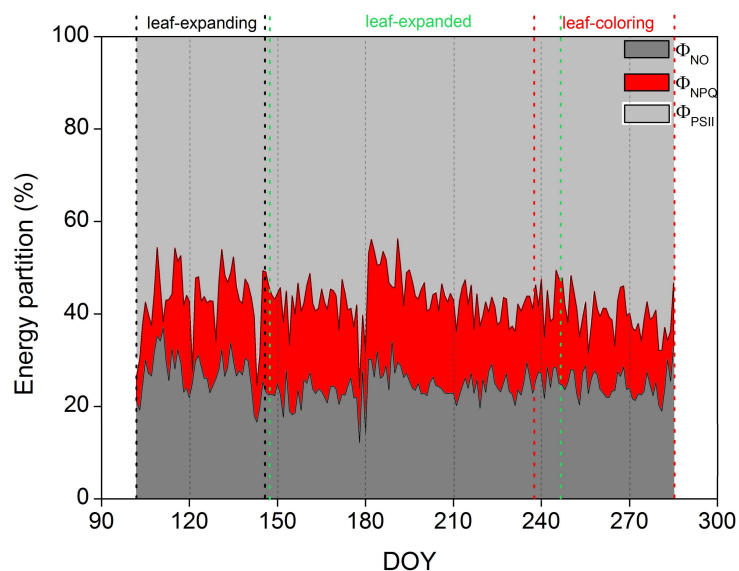


Figure 6. Timeseries of percentage of energy partitioning during the 2014 growing season. The red area is the quantum yield of regulatory (light-induced) energy dissipation (Φ_{NPQ}); the gray area is quantum yield of constitutive non-regulatory (basal or dark) energy dissipation (Φ_{NO}); and the light gray area is the quantum yield of light-induced photochemical quenching, which is equal to effective quantum yield of PSII photochemistry (Φ_{PSII}). Each phenophase is identified with a different color of dot lines.

Daily mean Φ_{NPQ} showed a correlation with PAR, T_a , and atmospheric water-related factors (i.e., RH and VPD; Figure 7). Daily mean Φ_{NPQ} decreased with increasing RH during the leaf-expanding and coloring phases (Figure 7a), whereas it increased with increasing VPD and PAR during the three phenophases (Figure 7b,c). Multivariate regressions showed PAR as the main controlling factor of Φ_{NPQ} during the three phenophases (Table 2).

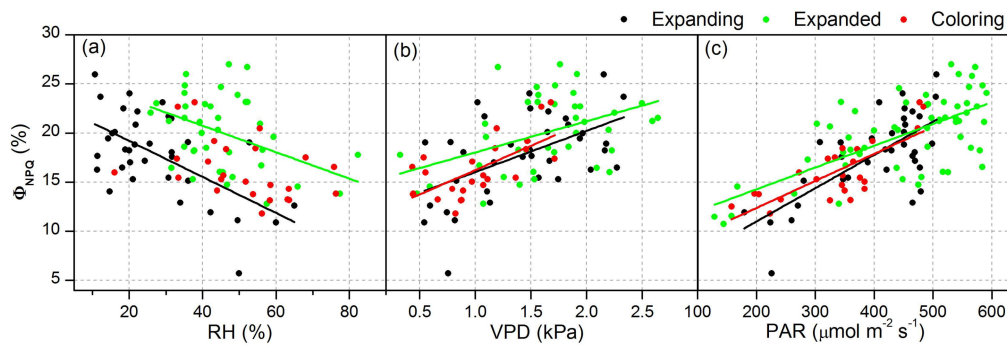


Figure 7. Response of quantum yield of regulatory light-induced non-photochemical quenching (Φ_{NPQ}) to daily mean air relative humidity (RH, (a)), atmospheric vapor pressure deficit (VPD, (b)), and incident photosynthetically active radiation (PAR, (c)) for each phenophase. Black, green, and red colored circles and lines coincide with values and fitting functions (Table 1) for the leaf-expanding, expanded, and coloring phases, respectively. Data from rainy days were excluded from the analysis.

4. Discussion

4.1. Effect of Environmental Stresses on F_v/F_m , Φ_{PSII} , and NPQ

Parameter F_v/F_m is commonly viewed as a reliable indicator of inhibition and of recovery from environmental stress. Variations in F_v/F_m can indicate photochemical regulation of PSII in response to stress [55]. Our results show that F_v/F_m fluctuated seasonally for 162 days of the 184 days of the growing season with a value below 0.80–0.83 in non-stressed environments [46,56–58]. Fluctuations coincided to inhibition by environmental stress and subsequent recovery as stress diminished (Figure 2). The inhibition occurred frequently in response to cold temperatures during the leaf-expanding and coloring phases and to summer drought during the leaf-expanded phase (Figures 1d and 2a). The shrubs were generally capable to recover to an optimal state when leaves were fully expanded (Figure 2). Presence of large fluctuations in F_v/F_m during spring implied greater inhibition during the leaf-expanding phase. A similar seasonal pattern in F_v/F_m to Φ_{PSII} indicated that stressful environmental conditions reduced both PSII photochemical capacity and efficiency. The averages of F_v/F_m for the three phenophases were 0.71 ± 0.08 , 0.76 ± 0.03 , and 0.76 ± 0.03 , close to the non-inhibition range, indicating *A. ordosica* can generally recover from inhibition and well adapted to the prevailing desert conditions.

Air temperature is a crucial factor affecting F_v/F_m or photochemical capacity during the leaf-expanding and coloring phases (Table 2, Figure 3a). The result that F_v/F_m linearly increased with increasing daily mean T_a (Figure 3a), indicated that photochemical capacity of PSII was downregulated by cold temperature during the early and late growing phases, suggesting probable low-temperature stress and capability of recovery as temperature increased. A similar relationship between F_v/F_m and ChlC indicated that the synthesis of chlorophyll coincided with an increase in photochemical capacity (Figure 3b). It is thus assumed that cold temperature during the early and late growing season reduced the chlorophyll content, thus reducing photochemical capacity and making the plant acclimatize to low temperatures. Some studies also reported that the PSII photochemical capacity of new leaves was often inhibited by a photo-oxidative cold-shock in early spring [59,60]. It was noted that cold temperature only reduced photochemical efficiency during the leaf-expanding rather than

leaf-coloring phase (Figures 3a and 4a). A reason for this may be due to physiological senescence around leaf coloration. The drastic changes of ChlC and Chl *a/b* was the result of the concomitant decrease of Chl *a* and *b* during the end of leaf expanded phase, with larger decrease in Chl *b* than Chl *a*, when PPT was high and temperature was low. These environmental conditions could activate the synthesis of abscisic acid [61] and induce the foliar defoliation process.

Variations in Φ_{PSII} reflected responsive sensitivity of the photosynthetic apparatus to abrupt ambient fluctuations [12]. Incident radiation has been shown to play an important role in modifying actual plant photochemical efficiency (Figure 4). Our results show that Φ_{PSII} decreased with increasing daily mean PAR during the three phenophases (Figure 4b), indicating that the reduction in photochemical efficiency was driven by excessive solar radiation during the growing season. Multivariate regression disclosed the changes in the relative role of PAR to T_a and VPD in affecting Φ_{PSII} during the leaf-expanding and expanded phases (Table 2), varying in opposing ways with PAR, T_a , and VPD controlling Φ_{PSII} during the leaf-expanding and expanded phases, respectively. Extreme temperatures were shown by some researchers to influence the fluidity and enzyme activity in and through the thylakoid membrane [62,63], thus dominating the acclimation of PSII to variable solar radiation during the leaf-expanding phase. Moreover, low temperature and high radiation could have a synergistic effect on photochemical efficiency when incident radiation increases beyond plant physiological needs on sunny days [64]. This can exacerbate reductions in photochemical efficiency compared to reductions associated with single stressors, leading to large reductions in photochemical capacity. Parameter NPQ decreased with increasing Chl *a/b* during the leaf-expanding and expanded phenophases (Figure 5), suggesting that the capacity of thermal dissipation through the consumption of excessive energy was regulated with changes in Chl *a* to Chl *b* content. This was because the majority of chlorophyll *b* is associated with light-harvesting complex proteins, which have an intrinsic ability to switch from an efficient light-harvesting state to a photo-protective state as a long-term strategy of acclimation to stressful conditions [65,66].

As a rule, low temperatures and high irradiance cause stress in plants during the leaf-expanding and expanded phenophases. However, plants are largely able to prevent and/or alleviate inhibition by thermal dissipation and regulation of changes in Chl *a* to Chl *b* content.

4.2. Acclimation of Energy Partitioning to Environmental Stresses

By dividing the Stern–Volmer NPQ parameter into quantum yield of regulatory and constitutive non-photochemical quenching, energy partitioning can provide quantitative information about the fraction of energy that is dissipated as heat [52,67]. The mean energy fraction of Φ_{PSII} in this study (i.e., 60%) was larger than that of the near 40% observed in some Mediterranean species [68,69], indicating a higher efficiency of energy utilization in *A. ordosica*. However, our result was slightly less than that of the approximately 65–73% for some plant species in mid-to-low latitude regions [51,70], due to the high inhibition observed at our site. Φ_{NO} values (Figure 6) in our study were generally within the range 20–30% reported for healthy green leaves [71], suggesting physiological resistance of *A. ordosica* during most of the growing season.

Energy partitioning was affected by the various abiotic factors. Low RH and high VPD was shown to produce high Φ_{NPQ} (Figure 7a,b), suggesting that the fraction of photo-protective thermal dissipation was increased as the air became drier. Water availability is reportedly one of the most common limitations to energy partitioning of incident radiation for arid and semi-arid plants [69]. The reason for water stress was presumably associated with low soil moisture induced stomata closure, increasing the trans-thylakoid proton gradient and mediating xanthophyll de-epoxidation, leading to increased protective thermal dissipation [72]. Specifically, during the leaf-expanding phase, RH was shown to explain more of the variation in Φ_{NPQ} than did VPD, assuming increasing photo-protection with dehydration stress. In contrast, due to the synergy of temperature and moisture, VPD explained more of the variation in Φ_{NPQ} than did RH during the leaf-coloring phase. We did not find significant correlations between soil water content and photosynthetic efficiency. This may be due to inadequate

water gradients and synergistic regulation by other meteorological factor (i.e., incident radiation and temperature). Further study is suggested to see how soil water content affects the photosynthetic efficiency by control experiment.

Incident radiation served as a controlling factor in the process of photosynthetic energy partitioning (Table 2). Parameter Φ_{NPQ} increased with increasing PAR in all phenophases (Figure 7c), suggesting that the fraction of photo-protective thermal dissipation was enhanced by relieving excitation pressure under conditions of excessive light. Some studies suggested that excitation pressure can be relaxed by the xanthophyll cycle, in which violaxanthin was de-epoxidated to zeaxanthin [73,74]. Concomitantly, excessive energy was dissipated and thylakoid pH difference was regulated to a moderate level. Reversible conversion between violaxanthin and zeaxanthin in the xanthophyll cycle can be viewed as a rapid response of the PSII system to variable irradiation.

In summary, the fraction of photosynthetic energy utilization and dissipation were dynamically regulated by simultaneous changes in the environment. Photosynthetic energy conversion can switch to a beneficial or protective state by regulating the relative changes in photochemical energy and thermal dissipation [75]. Through this regulation, plants can optimize the energy partitioning in a dynamic balance between the cost of photosynthetic utilization and the risk of photo-oxidative damage [76]. Strategy of dynamic acclimation can improve resistance to environmental extremes.

5. Conclusions

Inhibition happened throughout the growing season, being largely induced by cold air temperature (T_a) during the leaf-expanding and coloring phases and PAR in all phenophases. *A. ordosica* acclimated to stressful environmental conditions by way of non-photochemical quenching (NPQ) that was associated with reversible regulatory thermal dissipation and long-term regulation of relative decrease in Chl *a* to Chl *b* content. The fraction of thermal dissipation varied in response to PAR and atmospheric- and soil-water conditions. Thermal dissipation against excitation pressure fluctuated more greatly during the leaf-expanding phase relative to the leaf-expanded and coloring phases. *A. ordosica* was shown to undergo dynamic acclimation to changes in its external environment during most of its phenophases. Climate change may cause more extreme weather events in arid and semi-arid regions, leading to unfavorable environmental conditions for plant growth [77]. Our work added to the understanding of acclimation of desert species to changing climate. Further research is suggested to understand the acclamatory responses to various environmental stresses with different intensities and durations based on multi-year, continuous measurements of ChlF parameters.

Acknowledgments: We acknowledge the support obtained from National Natural Science Foundation of China (NSFC) (no. 31670710 and 31670708), the National Key Research and Development Program of China (no. 2016YFC0500905), and the Fundamental Research Funds for the Central Universities (no. 2015ZCQ-SB-02). We thank M. Y. Zhang, P. Liu, and S. J. Liu for their assistance with the field work. The U.S–China Carbon Consortium (USCCC) supported this work by way of helpful discussion and exchange of ideas. We greatly appreciate the valuable comments from all anonymous reviewers of this manuscript.

Author Contributions: T.Z. and X.J. designed the experiment; C.R. and Y.W. did the measurements, analyzed the data, and led the writing of the manuscript; C.P.-A.B., J.M., W.F., Y.B., and Y.T. discussed the results and contributed to the revision of the manuscript. All authors approved this manuscript for publication.

Conflicts of Interest: The authors declare no conflict of interest.

References

1. Ensminger, I.; Busch, F.; Huner, N. Photostasis and cold acclimation: Sensing low temperature through photosynthesis. *Physiol. Plant.* **2006**, *126*, 28–44. [[CrossRef](#)]
2. Yakushevskaya, A.E.; Jensen, P.E.; Keegstra, W.; van Roon, H.; Scheller, H.V.; Boekema, E.J.; Dekker, J.P. Supermolecular organization of photosystem II and its associated light-harvesting antenna in *Arabidopsis thaliana*. *FEBS. J.* **2001**, *268*, 6020–6028. [[CrossRef](#)]
3. Demmig-Adams, B.; Cohu, C.M.; Muller, O.; Adams, W.W. Modulation of photosynthetic energy conversion efficiency in nature: From seconds to seasons. *Photosynth. Res.* **2012**, 1–14. [[CrossRef](#)] [[PubMed](#)]

4. Ware, M.A.; Belgio, E.; Ruban, A.V. Photoprotective capacity of non-photochemical quenching in plants acclimated to different light intensities. *Photosynth. Res.* **2015**, *126*, 261–274. [[CrossRef](#)] [[PubMed](#)]
5. Zhou, Y.; Lam, H.M.; Zhang, J. Inhibition of photosynthesis and energy dissipation induced by water and high light stresses in rice. *J. Exp. Bot.* **2007**, *58*, 1207–1217. [[CrossRef](#)] [[PubMed](#)]
6. Müller, P.; Li, X.P.; Niyogi, K.K. Non-photochemical quenching. A response to excess light energy. *Plant Physiol.* **2001**, *125*, 1558–1566. [[CrossRef](#)] [[PubMed](#)]
7. Savitch, L.V.; Ivanov, A.G.; Gudynaite-Savitch, L.; Huner, N.P.; Simmonds, J. Effects of low temperature stress on excitation energy partitioning and photoprotection in *Zea mays*. *Funct. Plant Biol.* **2009**, *36*, 37–49. [[CrossRef](#)]
8. Porcar-castell, A.; Pfündel, E.; Korhonen, J.F.; Juurola, E. A new monitoring pam fluorometer (moni-pam) to study the short- and long-term acclimation of photosystem II in field conditions. *Photosynth. Res.* **2008**, *96*, 173–179. [[CrossRef](#)] [[PubMed](#)]
9. Durako, M.J. Using PAM fluorometry for landscape-level assessment of *Thalassia testudinum*: Can diurnal variation in photochemical efficiency be used as an ecoindicator of seagrass health? *Ecol. Indic.* **2012**, *18*, 243–251. [[CrossRef](#)]
10. Lazár, D. The polyphasic chlorophyll a fluorescence rise measured under high intensity of exciting light. *Funct. Plant Biol.* **2006**, *33*, 9–30. [[CrossRef](#)]
11. Harel, Y.; Ohad, I.; Kaplan, A. Activation of photosynthesis and resistance to photoinhibition in cyanobacteria within biological desert crust. *Plant Physiol.* **2004**, *136*, 3070–3079. [[CrossRef](#)] [[PubMed](#)]
12. Demmig-Adams, B.; Garab, G.; Adams, W., III; Govindjee. *Non-Photochemical Quenching and Energy Dissipation in Plants, Algae and Cyanobacteria*; Springer: Dordrecht, The Netherlands, 2014. [[CrossRef](#)]
13. Ruban, A.V. Nonphotochemical chlorophyll fluorescence quenching: Mechanism and effectiveness in protecting plants from photodamage. *Plant Physiol.* **2016**, *170*, 1903–1916. [[CrossRef](#)] [[PubMed](#)]
14. Adams, W.W., III; Muller, O.; Cohu, C.M.; Demmig-Adams, B. May photoinhibition be a consequence, rather than a cause, of limited plant productivity? *Photosynth. Res.* **2013**, *117*, 31–44. [[CrossRef](#)] [[PubMed](#)]
15. Haque, M.S.; Kjaer, K.H.; Rosenqvist, E.; Sharma, D.K.; Ottosen, C.O. Heat stress and recovery of photosystem II efficiency in wheat (*Triticum aestivum* L.) cultivars acclimated to different growth temperatures. *Environ. Exp. Bot.* **2014**, *99*, 1–8. [[CrossRef](#)]
16. Kalaji, H.M.; Jajoo, A.; Oukarroum, A.; Brestic, M.; Zivcak, M.; Samborska, I.A.; Cetner, M.D.; Łukasik, I.; Goltsev, V.; Ladle, R.J. Chlorophyll a fluorescence as a tool to monitor physiological status of plants under abiotic stress conditions. *Acta Physiol. Plant* **2016**, *38*, 102. [[CrossRef](#)]
17. Marias, D.E.; Meinzer, F.C.; Woodruff, D.R.; McCulloh, K.A. Thermo tolerance and heat stress responses of Douglas-fir and ponderosa pine seedling populations from contrasting climates. *Tree Physiol.* **2016**, *37*, 301–315. [[CrossRef](#)]
18. Öquist, G.; Huner, N.P. Photosynthesis of overwintering evergreen plants. *Annu. Rev. Plant Biol.* **2003**, *54*, 329–355. [[CrossRef](#)] [[PubMed](#)]
19. Liang, Y.; Chen, H.; Tang, M.J.; Yang, P.F.; Shen, S.H. Responses of *Jatropha curcas* seedlings to cold stress: Photosynthesis-related proteins and chlorophyll fluorescence characteristics. *Physiol. Plant.* **2007**, *131*, 508–517. [[CrossRef](#)] [[PubMed](#)]
20. Chaves, M.M.; Pereira, J.S.; Maroco, J.; Rodrigues, M.L.; Ricardo, C.P.P.; Osório, M.L.; Carvalho, I.; Faria, T.; Pinheiro, C. How plants cope with water stress in the field? Photosynthesis and growth. *Ann. Bot.* **2002**, *89*, 907–916. [[CrossRef](#)] [[PubMed](#)]
21. Ditmarová, L.; Kurjak, D.; Palmroth, S.; Kmeť, J.; Štřelcová, K. Physiological responses of Norway spruce (*Picea abies*) seedlings to drought stress. *Tree Physiol.* **2009**, *30*, 205–213. [[CrossRef](#)] [[PubMed](#)]
22. Suzuki, N.; Rivero, R.M.; Shulaev, V.; Blumwald, E.; Mittler, R. Abiotic and biotic stress combinations. *New Phytol.* **2014**, *203*, 32–43. [[CrossRef](#)] [[PubMed](#)]
23. Lazár, D.; Ilík, P.; Nauš, J. An appearance of K-peak in fluorescence induction depends on the acclimation of barley leaves to higher temperatures. *J. Lumin.* **1997**, *72*, 595–596. [[CrossRef](#)]
24. Niinemets, Ü. Responses of forest trees to single and multiple environmental stresses from seedlings to mature plants: Past stress history, stress interactions, tolerance and acclimation. *For. Ecol. Manag.* **2010**, *260*, 1623–1639. [[CrossRef](#)]

25. Gerganova, M.; Popova, A.V.; Stanoeva, D.; Velitchkova, M. Tomato plants acclimate better to elevated temperature and high light than to treatment with each factor separately. *Plant Physiol. Biochem.* **2016**, *104*, 234–241. [[CrossRef](#)] [[PubMed](#)]
26. Geist, H.J.; Lambin, E.F. Dynamic causal patterns of desertification. *AIBS Bull.* **2004**, *54*, 817–829. [[CrossRef](#)]
27. Ezcurra, E. *Global Deserts Outlook*; Scanprint: Aarhus, Denmark, 2006; ISBN 92-807-2722-2.
28. Lioubimtseva, E.; Henebry, G.M. Climate and environmental change in arid Central Asia: Impacts, vulnerability, and adaptations. *J. Arid. Environ.* **2009**, *73*, 963–977. [[CrossRef](#)]
29. Reynolds, J.F.; Smith, D.M.S.; Lambin, E.F.; Turner, B.L.; Mortimore, M.; Batterbury, S.P.; Huber-Sannwald, E. Global desertification: Building a science for dryland development. *Science* **2007**, *316*, 847–851. [[CrossRef](#)] [[PubMed](#)]
30. Chambers, J.C.; Bradley, B.A.; Brown, C.S.; D’Antonio, C.; Germino, M.J.; Grace, J.B.; Hardegree, S.P.; Miller, R.F.; Pyke, D.A. Resilience to stress and disturbance, and resistance to *Bromus tectorum* L. invasion in cold desert shrublands of western North America. *Ecosystems* **2014**, *17*, 360–375. [[CrossRef](#)]
31. Barker, D.H.; Adams, W.W.; Demmig-Adams, B.; Logan, B.A.; Verhoeven, A.S.; Smith, S.D. Nocturnally retained zeaxanthin does not remain engaged in a state primed for energy dissipation during the summer in two *Yucca* species growing in the Mojave Desert. *Plant Cell Environ.* **2002**, *25*, 95–103. [[CrossRef](#)]
32. Ogaya, R.; Penuelas, J.; Asensio, D.; Llusà, J. Chlorophyll fluorescence responses to temperature and water availability in two co-dominant Mediterranean shrub and tree species in a long-term field experiment simulating climate change. *Environ. Exp. Bot.* **2011**, *73*, 89–93. [[CrossRef](#)]
33. Xie, J.; Zha, T.; Jia, X.; Qian, D.; Wu, B.; Zhang, Y.; Bourque, C.P.-A.; Chen, J.; Sun, G.; Peltola, H. Irregular precipitation events in control of seasonal variations in CO₂ exchange in a cold desert-shrub ecosystem in northwest China. *J. Arid Environ.* **2015**, *120*, 33–41. [[CrossRef](#)]
34. Jia, X.; Zha, T.S.; Gong, J.N.; Wu, B.; Zhang, Y.Q.; Qin, S.G.; Chen, G.P.; Feng, W.; Kellomäki, S.; Peltola, H. Energy partitioning over a semi-arid shrubland in northern China. *Hydrol. Processes* **2016**, *30*, 972–985. [[CrossRef](#)]
35. Jiang, G.M.; Zhu, G.J. Different patterns of gas exchange and photochemical efficiency in three desert shrub species under two natural temperatures and irradiances in Mu Us Sandy Area of China. *Photosynthetica* **2001**, *39*, 257–262. [[CrossRef](#)]
36. Deng, W.H. Allelopathy of *Artemisia ordosica* Community in the Process of Plant Succession. Ph.D. Thesis. Beijing Forestry University, Beijing, China, 2016.
37. Porcar-Castell, A.; Juurola, E.; Ensminger, I.; Berninger, F.; Hari, P.; Nikinmaa, E. Seasonal acclimation of photosystem II in *Pinus sylvestris*. II. Using the rate constants of sustained thermal energy dissipation and photochemistry to study the effect of the light environment. *Tree. Physiol.* **2008**, *28*, 1483–1491. [[CrossRef](#)] [[PubMed](#)]
38. Repo, T.; Leinonen, I.; Ryyppö, A.; Finér, L. The effect of soil temperature on the bud phenology, chlorophyll fluorescence, carbohydrate content and cold hardiness of Norway spruce seedlings. *Physiol. Plant.* **2004**, *121*, 93–100. [[CrossRef](#)] [[PubMed](#)]
39. Qian, D.; Zha, T.S.; Wu, B.; Jia, X.; Qin, S.G. Spatio-temporal distribution characteristics of reference crop evapotranspiration in the Mu Us desert. *Acta Ecol. Sin.* **2017**, *37*, 1966–1974. [[CrossRef](#)]
40. Wilhelm, E.; Battino, R.; Wilcock, R.J. Low-pressure solubility of gases in liquid water. *Chem. Rev.* **1977**, *77*, 219–262. [[CrossRef](#)]
41. Chen, Z.H.; Zha, T.; Jia, X.; Wu, Y.; Wu, B.; Zhang, Y.; Guo, J.B.; Qin, S.G.; Chen, G.P.; Peltola, H. Leaf nitrogen is closely coupled to phenophases in a desert shrub ecosystem in China. *J. Arid. Environ.* **2015**, *122*, 124–131. [[CrossRef](#)]
42. Arnon, D.I. Copper enzymes in isolated chloroplasts. *Polyphenoloxidase in Beta vulgaris*. *Plant Physiol.* **1949**, *24*, 1. [[PubMed](#)]
43. Su, Z.S.; Zhang, X.Z. Comparison of determined methods of chlorophyll content. *Plant Physiol. J.* **1989**, *77*–78. [[CrossRef](#)]
44. Schreiber, U.; Schliwa, U.; Bilger, W. Continuous recording of photochemical and non-photochemical chlorophyll fluorescence quenching with a new type of modulation fluorometer. *Photosynth. Res.* **1986**, *10*, 51–62. [[CrossRef](#)] [[PubMed](#)]
45. Roháček, K. Chlorophyll fluorescence parameters: The definitions, photosynthetic meaning, and mutual relationships. *Photosynthetica* **2002**, *40*, 13–29. [[CrossRef](#)]

46. Zha, T.S.; Wu, Y.J.; Jia, X.; Zhang, M.Y.; Bai, Y.J.; Liu, P.; Ma, J.Y.; Bourque, C.-P. A.; Peltola, H. Diurnal response of effective quantum yield of PSII photochemistry to irradiance as an indicator of photosynthetic acclimation to stressed environments revealed in a xerophytic species. *Ecol. Indic.* **2017**, *74*, 191–197. [[CrossRef](#)]
47. Porcar-Castell, A. A high-resolution portrait of the annual dynamics of photochemical and non-photochemical quenching in needles of *Pinus sylvestris*. *Physiol. Plant.* **2011**, *143*, 139–153. [[CrossRef](#)] [[PubMed](#)]
48. Genty, B.; Harbinson, J. Regulation of light utilization for photosynthetic electron transport. In *Photosynthesis and the Environment*; Springer: Dordrecht, The Netherlands, 1996; Volume 5, pp. 67–99.
49. Cailly, A.L.; Rizzal, F.; Genty, B.; Harbinson, J. Fate of excitation at PSII in leaves, the nonphotochemical side. *Plant Physiol. Biochem.* **1996**, *86*, 28.
50. Kramer, D.M.; Johnson, G.; Kiirats, O.; Edwards, G.E. New fluorescence parameters for the determination of Q_A redox state and excitation energy fluxes. *Photosynth. Res.* **2004**, *79*, 209–218. [[CrossRef](#)] [[PubMed](#)]
51. Hendrickson, L.; Furbank, R.T.; Chow, W.S. A simple alternative approach to assessing the fate of absorbed light energy using chlorophyll fluorescence. *Photosynth. Res.* **2004**, *82*, 73. [[CrossRef](#)] [[PubMed](#)]
52. Lazár, D. Parameters of photosynthetic energy partitioning. *J. Plant Physiol.* **2015**, *175*, 131–147. [[CrossRef](#)] [[PubMed](#)]
53. Lazár, D. Chlorophyll *a* fluorescence induction. *BBA-Bioenerg.* **1999**, *1412*, 1–28. [[CrossRef](#)]
54. Oxborough, K.; Baker, N.R. Resolving chlorophyll *a* fluorescence images of photosynthetic efficiency into photochemical and non-photochemical components—calculation of qP and F_v/F_m without measuring F_o . *Photosynth. Res.* **1997**, *54*, 135–142. [[CrossRef](#)]
55. Maxwell, K.; Johnson, G.N. Chlorophyll fluorescence—A practical guide. *J. Exp. Bot.* **2000**, *51*, 659–668. [[CrossRef](#)] [[PubMed](#)]
56. Björkman, O.; Demmig, B. Photon yield of O_2 evolution and chlorophyll fluorescence characteristics at 77 K among vascular plants of diverse origins. *Planta* **1987**, *170*, 489–504. [[CrossRef](#)] [[PubMed](#)]
57. Lambers, H.; Chapin, F.S., III; Pons, T.L. *Plant Physiological Ecology*, 2nd ed.; Springer: Dordrecht, The Netherlands, 2008; pp. 39–40. [[CrossRef](#)]
58. Murchie, E.H.; Lawson, T. Chlorophyll fluorescence analysis: A guide to good practice and understanding some new applications. *J. Exp. Bot.* **2013**, *64*, 3983–3998. [[CrossRef](#)] [[PubMed](#)]
59. Kuk, Y.I.; Shin, J.S.; Burgos, N.R.; Hwang, T.E.; Han, O.; Cho, B.H.; Jung, S.; Guh, J.O. Antioxidative enzymes offer protection from chilling damage in rice plants. *Crop. Sci.* **2003**, *43*, 2109–2117. [[CrossRef](#)]
60. Pietrini, F.; Chaudhuri, D.; Thapliyal, A.P.; Massacci, A. Analysis of chlorophyll fluorescence transients in mandarin leaves during a photo-oxidative cold shock and recovery. *Agric. Ecosyst. Environ.* **2005**, *106*, 189–198. [[CrossRef](#)]
61. Baron, K.N.; Schroeder, D.F.; Stasolla, C. Transcriptional response of abscisic acid (ABA) metabolism and transport to cold and heat stress applied at the reproductive stage of development in *Arabidopsis thaliana*. *Plant Sci.* **2012**, *188–189*, 48–59. [[CrossRef](#)] [[PubMed](#)]
62. Ač, A.; Malenovský, Z.; Olejníčková, J.; Gallé, A.; Rascher, U.; Mohammed, G. Meta-analysis assessing potential of steady-state chlorophyll fluorescence for remote sensing detection of plant water, temperature and nitrogen stress. *Remote Sens. Environ.* **2015**, *168*, 420–436. [[CrossRef](#)]
63. Faik, A.; Popova, A.V.; Velitchkova, M. Effects of long-term action of high temperature and high light on the activity and energy interaction of both photosystems in tomato plants. *Photosynthetica* **2016**, *54*, 611–619. [[CrossRef](#)]
64. Wilhelm, C.; Selmar, D. Energy dissipation is an essential mechanism to sustain the viability of plants: The physiological limits of improved photosynthesis. *J. Plant Physiol.* **2011**, *168*, 79–87. [[CrossRef](#)] [[PubMed](#)]
65. Niyogi, K.K.; Truong, T.B. Evolution of flexible non-photochemical quenching mechanisms that regulate light harvesting in oxygenic photosynthesis. *Curr. Opin. Plant Biol.* **2013**, *16*, 307–314. [[CrossRef](#)] [[PubMed](#)]
66. Campos, H.; Trejo, C.; Peña-Valdivia, C.B.; García-Nava, R.; Conde-Martínez, F.V.; Cruz-Ortega, M.R. Photosynthetic acclimation to drought stress in *Agave salmiana* Otto ex Salm-Dyck seedlings is largely dependent on thermal dissipation and enhanced electron flux to photosystem I. *Photosynth. Res.* **2014**, *122*, 23–39. [[CrossRef](#)] [[PubMed](#)]
67. Bajkán, S.; Várkonyi, Z.; Lehoczki, E. Comparative study on energy partitioning in photosystem II of two *Arabidopsis thaliana* mutants with reduced non-photochemical quenching capacity. *Acta Physiol. Plant* **2012**, *34*, 1027–1034. [[CrossRef](#)]

68. Sperdouli, I.; Moustakas, M. Spatio-temporal heterogeneity in *Arabidopsis thaliana*, leaves under drought stress. *Plant Biol.* **2012**, *14*, 118–128. [[CrossRef](#)] [[PubMed](#)]
69. Osório, M.L.; Osório, J.; Romano, A. Photosynthesis, energy partitioning, and metabolic adjustments of the endangered Cistaceae species *Tuberaria major* under high temperature and drought. *Photosynthetica* **2013**, *51*, 75–84. [[CrossRef](#)]
70. Song, L.; Chow, W.S.; Sun, L.; Li, C.; Peng, C. Acclimation of photosystem II to high temperature in two *Wedelia* species from different geographical origins: Implications for biological invasions upon global warming. *J. Exp. Bot.* **2010**, *61*, 4087. [[CrossRef](#)] [[PubMed](#)]
71. Klughammer, C.; Schreiber, U. Complementary PSII quantum yields calculated from simple fluorescence parameters measured by PAM fluorometry and the saturation pulse method. *PAM Appl. Notes* **2008**, *1*, 27–35.
72. Flexas, J.; Bota, J.; Escalona, J.M.; Sampol, B.; Medrano, H. Effects of drought on photosynthesis in grapevines under field conditions: An evaluation of stomatal and mesophyll limitations. *Funct. Plant Biol.* **2002**, *29*, 461–471. [[CrossRef](#)]
73. Horton, P.; Johnson, M.P.; Perez-Bueno, M.L.; Kiss, A.Z.; Ruban, A.V. Photosynthetic acclimation: Does the dynamic structure and macro-organisation of photosystem II in higher plant grana membranes regulate light harvesting states? *FEBS. J.* **2008**, *275*, 1069–1079. [[CrossRef](#)] [[PubMed](#)]
74. Sacharz, J.; Giovagnetti, V.; Ungerer, P.; Mastroianni, G.; Ruban, A.V. The xanthophyll cycle affects reversible interactions between PsbS and light-harvesting complex II to control non-photochemical quenching. *Nat. Plants* **2017**, *3*, 16225. [[CrossRef](#)] [[PubMed](#)]
75. Terashima, I.; Hanba, Y.T.; Tazoe, Y.; Vyas, P.; Yano, S. Irradiance and phenotype: Comparative eco-development of sun and shade leaves in relation to photosynthetic CO₂ diffusion. *J. Exp. Bot.* **2005**, *57*, 343–354. [[CrossRef](#)] [[PubMed](#)]
76. Oguchi, R.; Hikosaka, K.; Hiura, T.; Hirose, T. Costs and benefits of photosynthetic light acclimation by tree seedlings in response to gap formation. *Oecologia* **2008**, *155*, 665. [[CrossRef](#)] [[PubMed](#)]
77. Donat, M.G.; Lowry, A.L.; Alexander, L.V.; O’Gorman, P.A.; Maher, N. More extreme precipitation in the world’s dry and wet regions. *Nat. Clim. Chang.* **2016**, *6*, 508–513. [[CrossRef](#)]



© 2018 by the authors. Licensee MDPI, Basel, Switzerland. This article is an open access article distributed under the terms and conditions of the Creative Commons Attribution (CC BY) license (<http://creativecommons.org/licenses/by/4.0/>).